Contribution from Christopher Ingold Laboratories,
University College London, London WC1H 0AJ, U.K.

Spectroscopic Studies on Linear-Chain Semiconductors and Related Species. Vibrational and Resonance Raman Spectroscopy of the Diphosphite Complexes $K_4[Pt_2(pop)_4]\cdot 2H_2O$, $K_4[Pt_2(pop)_4X_2]\cdot 2H_2O$, and $K_4[Pt_2(pop)_4X]\cdot nH_2O$, X = Cl, Br, I

MOHAMEDALLY KURMOO and ROBIN J. H. CLARK*

Received April 2, 1985

Electronic, infrared, Raman, and, in particular, resonance Raman studies of the diphosphite complexes $K_4[Pt_2(pop)_4]\cdot 2H_2O$, $K_4[Pt_2(pop)_4X_2]\cdot 2H_2O$, and $K_4[Pt_2(pop)_4X]\cdot nH_2O$, X = Cl, Br, I, have been carried out. The results provide independent confirmation of the assignment of the lowest allowed electronic transition of $K_4[Pt_2(pop)_4]\cdot 2H_2O$ to $^1A_{2u} \leftarrow {}^1A_{1g}$. The Raman spectra, in particular of $K_4[Pt_2(pop)_4I_2]\cdot 2H_2O$, consist of long, nearly harmonic progressions in ν_1 (ν(PtPt)) at resonance with the lowest electronic transition, reaching in this case as far as $12\nu_1$ ($\omega_1 = 105.0 \pm 0.5$ cm^{-1}, $x_{11} \leq 0.1$ cm^{-1}). The electronic spectra of the chain polymers, $K_4[Pt_2(pop)_4X]\cdot nH_2O$, are dominated at the low-wavenumber end by a $Pt^{III} \leftarrow Pt^{II}$ intervalence band in each case. Raman spectra taken at resonance with the intervalence band indicate that the chain chloride is a localized-valence species with very asymmetrically bridging chlorine atoms, as independently confirmed crystallographically. Both spectroscopic and crystallographic results indicate that the chain bromide and chain iodide are much more nearly delocalized valence species with nearly symmetric halogen bridges.

Introduction

The vibrational spectroscopy and, in particular, the resonance Raman (RR) spectroscopy of linear-chain semiconductors have proved to be immensely rich fields of study.[1] Typically, for halogen-bridged mixed-valence complexes of the Wolffram's red sort $[M^{II}L_4][M^{IV}L_4X_2][ClO_4]_4$ (Chart I), M = Pd, Pt, X = Cl, Br, I, L = amine, long progressions in the symmetric X–M^{IV}–X chain-stretching mode are observed in Raman spectra obtained with exciting lines whose wavelengths correspond to those of the chain $M^{IV} \leftarrow M^{II}$ intervalence transitions.[1,2] Attention has recently been directed to binuclear platinum diphosphite complexes which display interesting luminescence,[3,4] optical,[5] Raman, and infrared spectroscopy.[6-8] In particular, both we and Gray et al.[9] have recently synthesized a new type of semiconductor, $K_4[Pt_2(pop)_4X]\cdot nH_2O$, pop = $P_2O_5H_2^{2-}$ and X = Cl, Br, I, in which the average oxidation state of the platinum atoms is 2.5. These complexes form as golden metallic-looking crystals. The bromide has been found[9] to crystallize with a linear –Pt–Pt–Br–Pt–Pt–Br– chain along which the conductivity ($\sigma_\parallel$) is 10^{-4}–10^{-3} Ω^{-1} cm^{-1}, i.e. many orders of magnitude higher than that for complexes of the sort $[M^{II}L_4][M^{IV}L_4X_2][ClO_4]_4$ ($\sim 10^{-12}$–10^{-8} Ω^{-1} cm^{-1}).[1] The present investigation concentrates on the electronic, infrared, Raman, and, in particular, RR spectroscopy of the complexes $K_4[Pt_2(pop)_4]\cdot 2H_2O$, $K_4[Pt_2(pop)_4X_2]\cdot 2H_2O$, and $K_4[Pt_2(pop)_4X]\cdot nH_2O$, X = Cl, Br, I, and on the relation between the spectroscopy and structures of the complexes.[10,11]

Experimental Section

Preparations and Properties of Complexes. $K_4[Pt_2(pop)_4]\cdot 2H_2O$ was prepared as a green-yellow powder by published methods.[4] $K_4[Pt_2(pop)_4X_2]\cdot 2H_2O$, X = Cl, Br, I, was prepared by halogen oxidation of $K_4[Pt_2(pop)_4]\cdot 2H_2O$ in aqueous solution containing a slight excess of KX; the chloride, bromide, and iodide form yellow, orange, and brown crystals, respectively.

Chart I

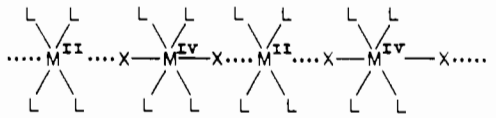

Table I. Electronic Spectra of Diphosphite Complexes in Aqueous Solution[a]

complex ion	λ_{max}/nm (ϵ_{max}/M^{-1} cm^{-1}) band III	band II	band I
$[Pt_2(P_2O_5H_2)_4]^{4-}$	367 (34 500)	452 (110)	
$[Pt_2(P_2O_5H_2)_4Cl_2]^{4-}$	282 (48 800)	345 (8200)	395 (w)
$[Pt_2(P_2O_5H_2)_4Br_2]^{4-}$	305 (55 400)	340 (11 800)	395 (sh?)
$[Pt_2(P_2O_5H_2)_4I_2]^{4-}$	338 (42 900)	435 (15 900)	

Band I: $E_u, A_{2u}(^3E_u) \leftarrow {}^1A_{1g}$ ($d_{\sigma^*} \leftarrow d_{\pi^*}$)
Band II: $E_u(^3A_{2u}) \leftarrow {}^1A_{1g}$ ($p_\sigma \leftarrow d_{\sigma^*}$) for $[Pt_2(pop)_4]^{4-}$; $E_u(^3A_{2u}) \leftarrow {}^1A_{1g}$ ($d_{\sigma^*} \leftarrow d_\sigma$) and $E_u(^1E_u) \leftarrow {}^1A_{1g}$ ($d_{\sigma^*} \leftarrow d_{\pi^*}$) for $[Pt_2(pop)_4X_2]^{4-}$
Band III: $A_{2u}(^1A_{2u}) \leftarrow {}^1A_{1g}$ ($p_\sigma \leftarrow d_{\sigma^*}$) for $[Pt_2(pop)_4]^{4-}$; $A_{2u}(^1A_{2u}) \leftarrow {}^1A_{1g}$ ($d_{\sigma^*} \leftarrow d_\sigma$) for $[Pt_2(pop)_4X_2]^{4-}$

[a] Assignments based on the electronic work of Che et al.[5] and the MCD work of Isci and Mason.[12]

$K_4[Pt_2(pop)_4X]\cdot nH_2O$ was prepared by partial oxidation of $K_4[Pt_2(pop)_4]\cdot 2H_2O$ with halogen in aqueous solution or by cocrystallizing equimolar amounts of $K_4[Pt_2(pop)_4]\cdot 2H_2O$ with $K_4[Pt_2(pop)_4X_2]\cdot 2H_2O$ in aqueous solutions containing a slight excess of KX. Large metallic gold crystals (1 × 1 × 0.5 mm) could be grown by the second method over a period of ca. 2 weeks. Elemental analyses for C, H, P, and X were satisfactory. These complexes revert to their constituent dimers on being dissolved in water.

Spectroscopic Measurements. Electronic absorption spectra of the complexes as aqueous solutions, KX pressed disks, or thin Nujol mulls were obtained at 295 K with a Cary 14 spectrometer.

Infrared spectra were recorded at 295 and 80 K with a Bruker 113V interferometer. Samples were prepared as pressed disks in the appropriate alkali halide for measurements between 4000 and 400 cm^{-1} and as wax disks for those between 600 and 20 cm^{-1}. The 4000–400-cm^{-1} spectrum of $K_4[Pt_2(pop)_4]\cdot 2H_2O$ was recorded as a Nujol mull (KBr plates) since in a pressed disk the complex reacts with the potassium halide under pressure, presumably forming mixed-valence (dark blue) complexes.

Raman spectra were recorded with a Spex 1401 double monochromator (1200 lines mm^{-1} Bausch and Lomb gratings) and a Spex 14018/R6 double/triple monochromator (1800 lines mm^{-1} Jobin-Yvon holographic gratings). Coherent Radiation Models CR3, CR 3000 K, and CR 12 lasers provided the exciting lines (337.1–752.5 nm). Detection of the scattered radiation was by photon-counting techniques using cooled RCA C31034 A photomultipliers. Samples were held as aqueous solutions (ca. 10^{-3} M), either stationary in capillary tubes or spinning (ca. 1000 rpm) in sealed tubes of diameter 2 cm. Complexes studied as solids were held as disks (KX, $K_2[SO_4]$, or $K[ClO_4]$) at ca. 80 K in a liquid-nitrogen Dewar assembly.

(1) Clark, R. J. H. *Adv. Infrared Raman Spectrosc.* **1984**, *11*, 95–132.
(2) Clark, R. J. H. *Chem. Soc. Rev.* **1984**, *13*, 219–244.
(3) Sperline, R. P.; Dickson, M. K.; Roundhill, D. M. *J. Chem. Soc., Chem. Commun.* **1977**, 62–63.
(4) Filomena Das Remedios Pinto, M. A.; Sadler, P. J.; Neidle, S.; Sanderson, M. R.; Subbiah, A. *J. Chem. Soc., Chem. Commun.* **1980**, 13–15.
(5) Che, C.-M.; Schaefer, W. P.; Gray, H. B.; Dickson, M. K.; Stein, P.; Roundhill, D. M. *J. Am. Chem. Soc.* **1982**, *104*, 4253–4255.
(6) Stein, P.; Dickson, M. K.; Roundhill, D. M. *J. Am. Chem. Soc.* **1983**, *105*, 3489–3494.
(7) Clark, R. J. H.; Kurmoo, M. *J. Chem. Soc., Dalton Trans.* **1985**, 579–585.
(8) Clark, R. J. H. Plenary lecture, Conference, Electrical and Magnetic Properties of Low Dimensional Solids, The Royal Society, June 1984.
(9) Che, C.-M.; Herbstein, F. H.; Schaefer, W. M.; Marsh, R. E.; Gray, H. B. *J. Am. Chem. Soc.* **1983**, *105*, 4604–4607.
(10) Marsh, R. E.; Herbstein, F. H. *Acta Crystallogr., Sect. B: Struct. Crystallogr. Cryst. Chem.* **1983**, *B39*, 280–287.
(11) Clark, R. J. H.; Kurmoo, M.; Dawes, H. M.; Hursthouse, M. B., submitted for publication.

0020-1669/85/1324-4420$01.50/0

Laser power at the sample was held at <50 mW. Wavenumber calibration was effected by reference to the emission spectrum of neon. Intensities were estimated by measurements of (peak heights) × (full widths at half-maximum), averaged for three to five separate measurements and corrected for the spectral response of the instrument. The a_1 band of $[ClO_4]^-$ was used as internal standard.

Polarized RR spectra of single crystals of $K_4[Pt_2(pop)_4Cl]\cdot 3H_2O$ were obtained at 15 K by use of an Air Products Displex cryostat. Laser power at the crystals was held to <10 mW. The crystals (ca. 0.7 × 0.5 × 0.5 mm^3) were aligned under a polarizing microscope and glued onto a copper block, which was then attached to the cryostat.

ESR spectra were recorded between 295 and 120 K with a Varian E4 spectrometer, microcrystalline samples being held in Lindemann tubes.

Results and Discussion

The electronic spectra of the discrete species (all approximately of D_{4h} symmetry) $[Pt_2(pop)_4]^{4-}$ and $[Pt_2(pop)_4X_2]^{4-}$, X = Cl, Br, I (Table I), are closely similar to those recently obtained by Isci and Mason[12] in the course of a magnetic circular dichroism (MCD) study. The MCD terms for the 452- and 367-nm bands of the platinum(II) species $[Pt_2(pop)_4]^{4-}$ indicate that the appropriate assignments for these bands are $E_u(^3A_{2u}) \leftarrow {}^1A_{1g}$ and $^1A_{2u} \leftarrow {}^1A_{1g}$, respectively, the excited states being derived from the $d_{\sigma^*}p_\sigma$ ($5d_{z^2}6p_z$) configuration. The two low-energy bands of the platinum(III) species $[Pt_2(pop)_4X_2]^{4-}$ are attributed to $d_{\sigma^*} \leftarrow d_{\pi^*}$ and $d_{\sigma^*} \leftarrow d_\sigma$ type transitions (Table I). The spectra of these dimers as KX disks are virtually identical with those taken on aqueous solutions. The electronic spectra of the chain complexes have not previously been reported, but they are expected to involve intervalence transitions[2] at low wavenumbers.

The principal structural change associated with platinum-based transitions of the $p_\sigma \leftarrow d_{\sigma^*}$, $d_{\sigma^*} \leftarrow d_{\pi^*}$, or $d_{\sigma^*} \leftarrow d_\sigma$ sort is expected to be a change in the Pt–Pt bond length. Hence, at resonance with any band so attributed, a progression in ν(Pt–Pt) is expected to be the dominant feature of the Raman spectrum.[13] The following results give clear evidence that this is the case.

$K_4[Pt_2(pop)_4]\cdot 2H_2O$. RR spectra of $K_4[Pt_2(pop)_4]\cdot 2H_2O$ in aqueous solution have been obtained previously,[14] for the species both in the ground state and (by time-resolved resonance Raman (TR^3) techniques) in its $^3A_{2u}$ ($d_{\sigma^*}p_\sigma$) state.[15] The ground-state spectrum (356.4-nm excitation) consisted solely of a progression to three members in a band attributed to ν(PtPt). The present investigation was based on a RR study of the solid complex in a $K[ClO_4]$ matrix also using 356.4-nm excitation, i.e. at resonance with the 367-nm band. Two progressions in ν_1 (ν(PtPt)) are observed under these conditions (Table II), $v_1\nu_1$ as far as $v_1 = 5$ and $v_1\nu_1 + 263$ as far as $v_1 = 2$, where the 263-cm^{-1} band is probably attributable to a ring bending mode. The anharmonicity constant $x_{11} \leq 1$ cm^{-1}. These results demonstrate the increased quality of RR spectra obtainable at low temperatures and confirm that the principal structural change in the complex associated with an electronic transition at 367 nm is along (and, on the basis of molecular orbital arguments, a contraction along) the PtPt coordinate. Although the complex was studied with a range of exciting lines (514.5–337.1 nm), the excitation profile of ν_1 could not be obtained owing to strong emission.

Aqueous solution measurements with 356.4- or 350.7-nm excitation reveal an RR progression in ν_1 to four members (117, 234, 350, and 465 cm^{-1}), all of which are polarized and therefore, as expected, attributable to totally symmetric modes (as ν_1 and its overtones must be). The depolarization ratio of ν_1 at resonance with the 367-nm band is $^1/_3$, a result which indicates that the resonant transition is z-polarized.[13,14] This is the polarization expected for a $^1A_{2u} \leftarrow {}^1A_{1g}$ transition, and thus the result provides independent confirmation in all respects of the assignments of Gray et al.[15,16] and Isci and Mason.[12]

$K_4[Pt_2(pop)_4X_2]\cdot 2H_2O$. The basic spectral data on, and vibrational analysis for, the $[Pt_2(pop)_4X_2]^{4-}$ ions have been obtained by Stein et al.[17] The present investigation therefore concentrates on the RR study.

Table II. Wavenumbers and Assignments of Bands Observed in the Resonance Raman Spectra of Binuclear Diphosphite Species

$\tilde{\nu}$/cm^{-1}	assignt	$\tilde{\nu}$/cm^{-1}	assignt
	$K_4[Pt_2(pop)_4]\cdot 2H_2O$[a] ($\lambda_0$ = 356.4 nm)		
115 vs	ν_1' ($\nu(Pt^{II}–Pt^{II})$)	373 w	$\nu_1' + 263$
231 s	$2\nu_1'$	458 wm	$4\nu_1'$
263 w	ring bending	490 vw	$2\nu_1' + 263$
345 m	$3\nu_1'$	570 w	$5\nu_1'$
	$K_4[Pt_2(pop)_4Cl_2]\cdot 2H_2O$[b] ($\lambda_0$ = 356.4 nm)		
158 vs	ν_1 ($\nu(Pt^{III}–Pt^{III})$)	305 s	ν_2 ($\nu(Pt^{III}–Cl)$)
	$K_4[Pt_2(pop)_4Br_2]\cdot 2H_2O$[a,b] ($\lambda_0$ = 356.4 nm)		
133	ν_1 ($\nu(Pt^{III}–Pt^{III})$)	223	ν_2 ($\nu(Pt^{III}–Br)$)
	$K_4[Pt_2(pop)_4I_2]\cdot 2H_2O$[c] ($\lambda_0$ = 482.5 nm)		
105.4 vvs	ν_1 ($\nu(Pt^{III}–Pt^{III})$)	629 w	$6\nu_1$
189.1 w	ν_2 ($\nu(Pt^{III}–I)$)	655 vw	$3\nu_1 + \nu_3$
209.9 vs	$2\nu_1$	734 w	$7\nu_1$
294.2 w	$\nu_1 + \nu_2$	760 vw	$4\nu_1 + \nu_3$
314.7 s	$3\nu_1$	839 w	$8\nu_1$
340 w	ν_3 ($\nu(Pt^{III}–P)$)	865 vw	$5\nu_1 + \nu_3$
399 vw	$2\nu_1 + \nu_2$	948 vw	$9\nu_1$
419.2 m	$4\nu_1$	970 vw	$6\nu_1 + \nu_3$
445 vw	$\nu_1 + \nu_3$	1050 vw	$10\nu_1$
504 vw	$3\nu_1 + \nu_2$	1075 vw	$7\nu_1 + \nu_3$
524.2 m	$5\nu_1$	1155 vw	$11\nu_1$
550 vw	$2\nu_1 + \nu_3$	1260 vw	$12\nu_1$
608 vw	$4\nu_1 + \nu_2$		

[a] $K[ClO_4]$ disk matrix held at ca. 80 K. [b] Aqueous solution at 295 K. [c] KI disk matrix held at ca. 80 K.

The Raman spectra (λ_0 = 514.5 nm) of $K_4[Pt_2(pop)_4X_2]\cdot 2H_2O$, X = Cl, Br, in aqueous solution consist in each case of a two-band pattern at 158, 305 (X = Cl) and 133, 223 (X = Br) cm^{-1}. The 158- and 133-cm^{-1} bands are, as previously,[17] assigned to ν_1 (ν(PtPt)) and the 305- and 223-cm^{-1} bands to ν_2 (ν(PtX)). Excitation with 457.9-, and 356.4-, and 350.7-nm lines causes decomposition of these complexes to $[Pt_2(pop)_4]^{4-}$, as evidenced by the development of phosphorescence centered on 19 500 cm^{-1} and of an intense Raman band at 117 cm^{-1}. The decomposition of these ions could be reduced substantially by holding the samples as $K[ClO_4]$ disks at ca. 80 K or as the salts $[Pt(en)_2][Pt(en)_2X_2][Pt_2(pop)_4X_2]$, en = 1,2-diaminoethane, as $K_2[SO_4]$ disks at ca. 80 K.[7] However, the available exciting lines were not sufficiently near in wavelength to the electronic band maxima of the ions to permit excitation profiles of ν_1 and ν_2 to be obtained.

Although the analogous iodide (ν_1 = 110, ν_2 = 192 cm^{-1} in aqueous solution) was likewise not stable sufficiently long in solution for either excitation profile or ρ-value measurements, no decomposition was detected when it was held as a KI disk at ca. 80 K. Under the latter conditions and with λ_0 = 476.5 nm, the RR spectrum of the iodide displays three progressions, viz. $v_1\nu_1$, $v_1\nu_1 + \nu_2$, and $v_1\nu_1 + \nu_3$, reaching v_1 = 12, 5, and 7, respectively, where ν_1 (ν(PtPt)) and ν_2 (ν(PtI)) occur at 105 and 189 cm^{-1}, respectively. The ν_3 mode (340 cm^{-1}) is assigned (Table II) to ν(PtP). The ν_1 mode is harmonic within experimental error, standard analysis yielding $\omega_1 = 105.0 \pm 0.5$ cm^{-1} and $x_{11} = 0.0 \pm 0.1$ cm^{-1}.

The excitation profile of ν_1 of $[Pt_2(pop)_4I_2]^{4-}$ could be followed for a variety of exciting lines in the 450–550-nm region. Since this profile maximizes at 500 nm, ν_1 is clearly coupled to the x,y-polarized transitions centered on 435 nm. However, the substantial red shift (3000 cm^{-1}) of the maximum relative to the absorption band maximum indicates the presence of strong interference between the two transitions (Table I) centered around 435 nm. The interference appears similar to that observed between the $^1T_2$ and $^1T_1$ contributions to the transition polarizability for

(12) Isci, H.; Mason, W. R. *Inorg. Chem.* **1985**, *24*, 1761–1765.
(13) Clark, R. J. H. *Adv. Chem. Ser.* **1983**, *No. 211*, 509–514.
(14) Mortensen, O. S.; Hassing, S. *Adv. Infrared Raman Spectrosc.* **1980**, *6*, 1–60.
(15) Che, C.-M.; Butler, L. G.; Gray, H. B.; Crooks, R. M.; Woodruff, W. H. *J. Am. Chem. Soc.* **1983**, *105*, 5492–5494.
(16) Rice, S. F.; Gray, H. B. *J. Am. Chem. Soc.* **1983**, *105*, 4571–4575.
(17) Stein, P.; Dickson, M. K.; Roundhill, D. M. *J. Am. Chem. Soc.* **1983**, *105*, 3489–3494.

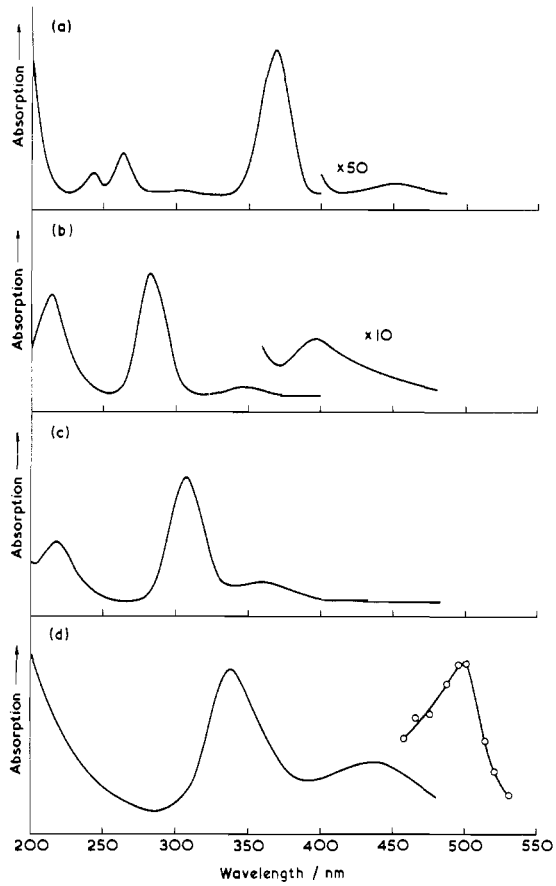

Figure 1. Electronic absorption spectra of (a) $K_4[Pt_2(pop)_4]\cdot 2H_2O$, (b) $K_4[Pt_2(pop)_4Cl_2]\cdot 2H_2O$, (c) $K_4[Pt_2(pop)_4Br_2]\cdot 2H_2O$, and (d) $K_4[Pt_2(pop)_4I_2]\cdot 2H_2O$ in water at 295 K, together with the excitation profile (O) of the ν(PtPt) fundamental of the iodide measured at ca. 80 K.

Chart II

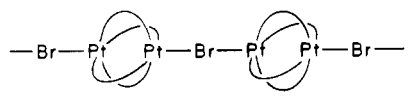

the a_1 band of $[WS_4]^{2-}$.[18] The ν_2 band is insufficiently intense for measurements of its excitation profile to be made (Figure 2).

The bromo ion, $[Pt_2(pop)_4Br_2]^{4-}$, displays intense red luminescence centered on ca. 13 000 cm^{-1}, similar to that observed for $[Pt(en)_2][Pt(en)_2Br_2][Pt_2(pop)_4Br_2]$.[7]

$K_4[Pt_2(pop)_4X]\cdot nH_2O$. The metallic gold reflection of the complexes $K_4[Pt_2(pop)_4X]\cdot nH_2O$, X = Cl, Br, I, are strikingly reminiscent of the appearance of Wolffram's red type salts, the colors of which are due primarily to strong, very broad, intervalence bands lying in the region 10 000–25 000 cm^{-1}. The implied structural analogy between these different classes of mixed-valence complex is broadly borne out by the X-ray crystallographic results of Gray and co-workers,[9] who have shown that the bromide does indeed crystallize with a chain structure (Chart II). Their results implied that the bridging bromine atoms were centrally placed between the $Pt_2(pop)_4$ units, a conclusion that would account for the high observed chain conductivity but one that would be surprising in view of the expected Peierls instability of symmetric linear chains (though any Peierl's distortion may only occur well below the (room) temperature at which the crystallography was carried out). Further, the symmetric PtBr stretching mode would be Raman-inactive were the bromine atoms centrally placed. Accordingly, it seemed important to investigate the spectroscopy of these mixed-valence complexes both in its own right as well as for the provision of structural pointers.

The electronic spectra of the complexes (Table III) as Nujol mulls at 295 K are, in each case, dominated by a very intense and

Table III. Electronic Spectra of Chain Diphosphite Complexes[a] (λ_{max}/nm)

complex	other metal-based transitions			intervalence band
$K_4[Pt_2(pop)_4Cl]\cdot 3H_2O$	287	355	390	512
$K_4[Pt_2(pop)_4Br]\cdot 3H_2O$	310	355	385	645
$K_4[Pt_2(pop)_4I]\cdot nH_2O$	330	370	460	870

[a] Measured as Nujol mulls at 295 K.

Chart III

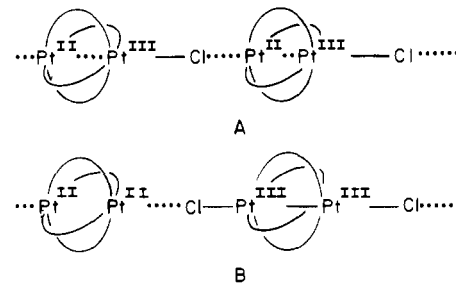

Chart IV

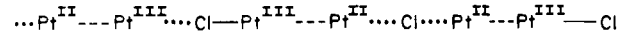

very broad band centered at 19 500, 15 500, and 11 400 cm^{-1} for X = Cl, Br, and I, respectively. In all its characteristics (wavenumber, intensity, and breadth), this band behaves like an intervalence band of a halogen-bridged species, and it is accordingly so assigned. The higher energy bands likewise appear to be d–d transitions of the $Pt_2(pop)_4$ units (cf. earlier discussion), but in the absence of single-crystal data, firm assignments cannot be made.

The Raman spectrum of $K_4[Pt_2(pop)_4Cl]\cdot 3H_2O$ at resonance with the intervalence transition (Figure 5) is dominated by a band at 291 cm^{-1}, which is readily attributable to ν_2 (ν(PtCl)), somewhat lowered (on account of bridging) from its value (305 cm^{-1}) for the discrete species $[Pt_2(pop)_4Cl_2]^{4-}$ (vide supra). The longest progressions observed at resonance also involve ν_2 ($\upsilon_2\nu_2$ to υ_2 = 6, $\nu_1 + \upsilon_2\nu_2$ to υ_2 = 5, $\nu_1' + \upsilon_2\nu_2$ to υ_2 = 3, and $\nu_2' + \upsilon_2\nu_2$ to υ_2 = 3), clearly indicating that the principal structural change on excitation to the intervalence state is along the Pt–Cl coordinate (which is clearly totally symmetric; see Figure 6). The complexes are therefore directly analogous to Wolffram's red type salts in this respect. The other modes involved in these progressions are ν_1 (ν(PtPt)), ν_1' (for which no assignment is offered), and ν_2', which is assigned to a ring bending mode[17] (cf. analogous assignment for the 263-cm^{-1} band of the discrete species $[Pt_2(pop)_4]^{4-}$ (vide supra)).

There is an even more important conclusion to be drawn from these RR results, i.e. that the chlorine atom cannot be centrally bridging between the $Pt_2(pop)_4$ units, otherwise the ν_2 mode would be Raman-inactive. Thus, there are two possible structures for the chain (see Chart III). These possibilities may in principle be distinguished by consideration of the infrared spectrum of the complex. However, this point is difficult to resolve in practice owing (a) to overlapping bands (Table V) and (b) to the poor mulling properties of (and thus spectrum given by) the sample. The infrared spectrum suggests that ν_2 is weakly infrared-active and virtually coincident with its Raman value, a result that would only be consistent with structure A. Stronger evidence that $K_4[Pt_2(pop)_4Cl]\cdot 3H_2O$ consists of a stacked polar dimer (structure A) with noncentrally placed chlorine atom bridges has been obtained by X-ray crystallography,[11] the $Pt^{III}Cl$ and $Pt^{II}\cdots Cl$ distances differing by 0.599 Å.

Transition to the intervalence state would produce the following Pt^{III}/Pt^{II} entity along the Pt^{II}/Pt^{III} chain (Chart IV) i.e. one in which substantial chlorine atom movement is required (as implied by the RR results), but since there is no change in Pt···Pt bond order ($^1/_2$ in each state), little if any change in Pt–Pt bond length is required. Consistent with the latter, although ν_1 (ν(PtPt)) gives rise to an intense band at 152 cm^{-1} in the RR spectrum, it does

(18) Clark, R. J. H.; Dines, T. J.; Proud, G. P. *J. Chem. Soc., Dalton Trans.* **1983**, 2019–2024.

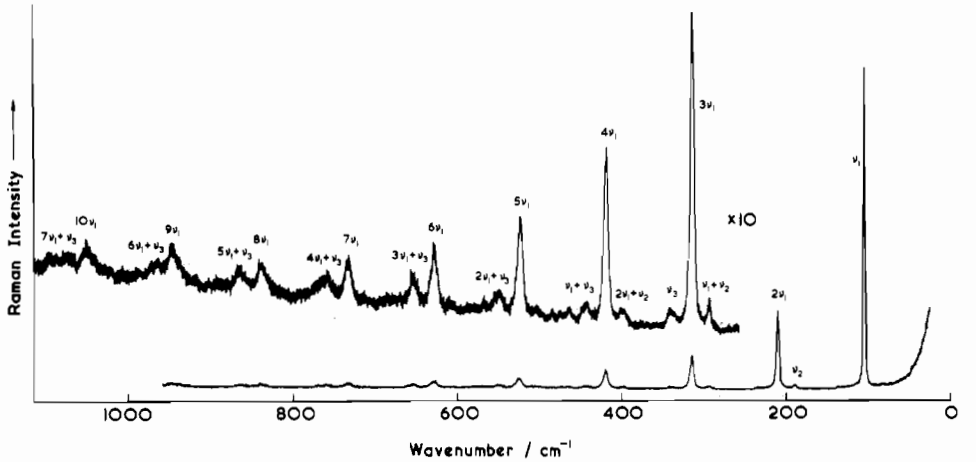

Figure 2. Resonance Raman spectrum of $K_4[Pt_2(pop)_4I_2]\cdot 2H_2O$ as a KI disk at ca. 80 K (λ_0 = 482.5 nm, power 30 mW, slit widths 100/500/100 μm).

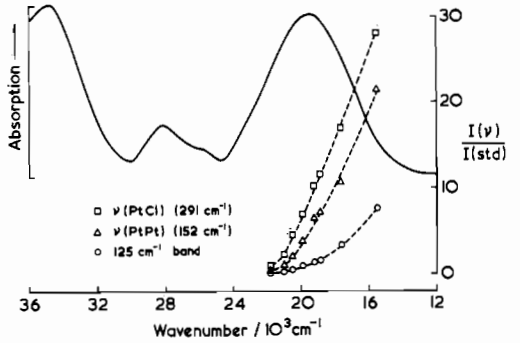

Figure 3. Electronic absorption spectrum of $K_4[Pt_2(pop)_4Cl]\cdot 3H_2O$ measured as a Nujol mull at 295 K, together with the excitation profiles of the ν(PtCl) (□, ν_2), ν(PtPt) (Δ, ν_1) and 125 (○, ν_1') bands.

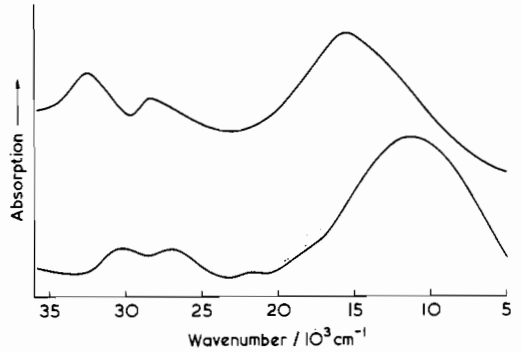

Figure 4. Electronic absorption spectra of $K_4[Pt_2(pop)_4Br]\cdot 3H_2O$ (top) and $K_4[Pt_2(pop)_4I]\cdot nH_2O$ (bottom) measured as Nujol mulls at 295 K.

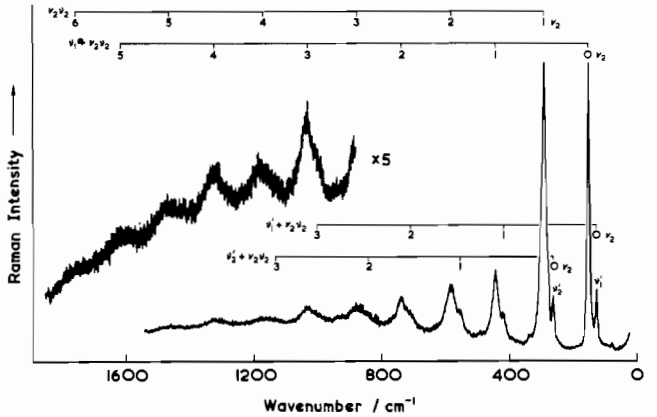

Figure 5. Resonance Raman spectrum of $K_4[Pt_2(pop)_4Cl]\cdot 3H_2O$ as a $K[ClO_4]$ disk at ca. 80 K (λ_0 = 647.1 nm, power 20 mW, spectral slit width 1.7 cm^{-1}).

not give a progression of the sort $\nu_1\nu_1$. The RR results are included in Table IV together with various other band assignments.

Table IV. Wavenumbers and Assignments of Bands Observed in the Resonance Raman Spectra of Chain Platinum Diphosphite Complexes[a]

$\tilde{\nu}$/cm^{-1}	assignt	$\tilde{\nu}$/cm^{-1}	assignt
	$K_4[Pt_2(pop)_4Cl]\cdot 3H_2O$ (λ_0 = 647.1 nm)		
78 w	...	583 ms	$2\nu_2$
125.8 wm	ν_1'	710 sh br	$\nu_1' + 2\nu_2$
152.3 vs	ν_1 (ν(PtPt))	735 sh w	$\nu_1 + 2\nu_2$
263 wm	ν_2'	843 sh	$\nu_2' + 2\nu_2$
279 vw sh	$\nu_1' + \nu_1$	874 m	$3\nu_2$
291.3 vs	ν_2 (ν(PtCl))	997 sh	$\nu_1' + 3\nu_2$
339 w	ν(PtP)	1027 m	$\nu_1 + 3\nu_2$
397 vw, ?	$2\nu_1' + \nu_1$	1135 sh	$\nu_2' + 3\nu_2$
418 w	$\nu_1' + \nu_2$	1165 w	$4\nu_2$
443 ms	$\nu_1 + \nu_2$	1318 w, br	$\nu_1 + 4\nu_2$
490 w	$\nu_1 + \nu$(PtP)	1460 w, br	$5\nu_2$
552 w	$\nu_2' + \nu_2$	1600 w, br	$\nu_1 + 5\nu_2$
		1745 vw, br	$6\nu_1$
	$K_4[Pt_2(pop)_4Br]\cdot 3H_2O$ (λ_0 = 647.1 nm)		
93 w	δ(PtPtBr)	223 w	
117 vs	ν_1 (ν(PtPt))	239 m	$2\nu_1$
122 vs		330 wm	$\nu_1 + \nu_2$
137 wm		355 wm	$3\nu_1$
195 wm		450 w, br	$2\nu_1 + \nu_2$
210 m	ν_2 (ν(PtBr))	475 w, br	$4\nu_1$
	$K_4[Pt_2(pop)_4I]\cdot nH_2O$ (λ_0 = 676.4 nm)		
85 vw	δ(PtPtI)	395 wm	$4\nu_1$
100 vs	ν_1 (ν(PtPt))	493 w	$5\nu_1$
126 w sh		737 wm	δ(POP)
185 w sh	ν(PtI)	837 w	$\nu_1 + \delta$(POP)
199 s	$2\nu_1$	935 w	$2\nu_1 + \delta$(POP)
296 m	$3\nu_1$		

[a] $K[ClO_4]$ disk matrix held at ca. 80 K.

The excitation profiles of the ν_1 and ν_2 bands both increase enormously to the red of the intervalence band; the actual maxima were not located but are at least 4000 cm^{-1} red shifted from that of the intervalence band. This behavior is typical of that of the symmetric PtCl stretching mode of any Wolffram's red type salt, the excitation profiles of which are known to maximize at the band edge rather than the band maximum of semiconductors.[1] The 263-cm^{-1} band (considered to be a ring-bending mode) is also slightly resonance enhanced.

The RR spectrum of $K_4[Pt_2(pop)_4Br]\cdot 3H_2O$ (Figure 7) is similar to that of the analogous chloride except that no overtones of ν_2, the symmetric PtBr stretching mode, were observed. This implies that any structural change along the Pt–Br coordinate on excitation to the intervalence state must be very small in this case. This is consistent with the X-ray result on the complex, except that, for this mode to give rise to a Raman band at all must imply that the bromine atom cannot be located precisely at the central position of the bridge (it is not strictly required to do so in the space group $P4/mbm$ in which the complex crystallizes). The

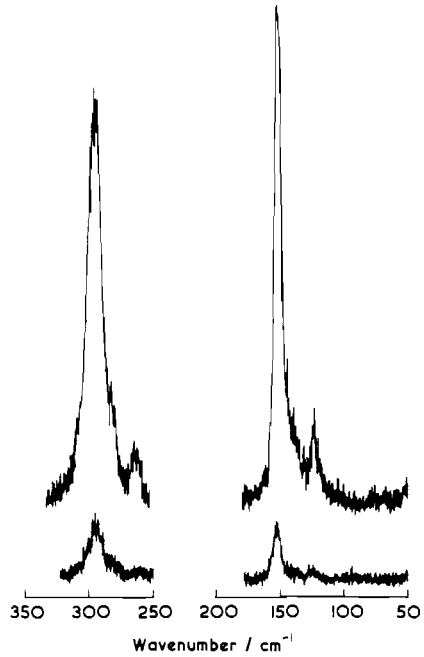

Figure 6. Resonance Raman spectra of a single crystal of $K_4[Pt_2(pop)_4Cl]\cdot 3H_2O$ at ca. 15 K (λ_0 = 647.1 nm, power <10 mW, spectral slit width 2 cm^{-1}). Top and bottom spectra relate to the $y(zz)x$ and $y(zy)x$ orientations, respectively.

Table V. Infrared Spectra (560–80 cm^{-1}) of $K_4[Pt_2(pop)_4X]\cdot nH_2O$ at ca. 80 K

X			
Cl	Br	I	assignt[a]
98 w	102 w	104 m	
	120 w	117 m	
130 m	143 m	144 m sh	
155 w	157 m	153 s	
171 w	185 m	184 m	
187 m	194 m	197 m	
240 s	239 s	240 s	ring bending
261 w	259 m	267 wm	
	263 m		
281 w sh	276 m	276 ms	ring bending
290 m	293 wm	291 wm	ring bending/ ν(PtCl)?
310 w	308 w	308 m	ν(PtP)/ring bending
320 m	315 w	316 m	
	325 s	325 s	
339 vs	335 m	335 ms	
	342 m	341 ms	
352 vw sh	352 wm	352 wm	
362 w	359 w	360 w	
~400 w sh	410 m	408 s	PO_2 bending
431 w sh	434 w sh	430 w sh	
449 vs	448 vs	446 m	
464 m	465 vs	461 vs	
494 m, br	492 m, br	493 w	
	511 s	512 s	
525 vs	537 s	534 s	
553 m sh	556 s	555 s	

[a] Based on assignments for related monomeric species. The spectra of the bromide and iodide are very similar to one another but differ slightly from that of the chloride.

ν_2 value (210 cm^{-1}) is 13 cm^{-1} less than that for the $[Pt_2(pop)_4Br_2]^{4-}$ ion as a consequence of bridging. The longest observed progression in this case is in ν_1 (to $4\nu_1$), where ν_1 is the PtPt stretching mode at ca. 120 cm^{-1}. The spectroscopic and crystallographic result that the bridging chlorine atom is much more asymmetrically placed than is the bridging bromine atom in these complexes is also mirrored exactly in that obtained for Wolffram's red type salts.[1]

Similar results were obtained for $K_4[Pt_2(pop)_4I]\cdot nH_2O$. No overtones of ν_2, the PtI stretching mode at 185 cm^{-1}, were detected,

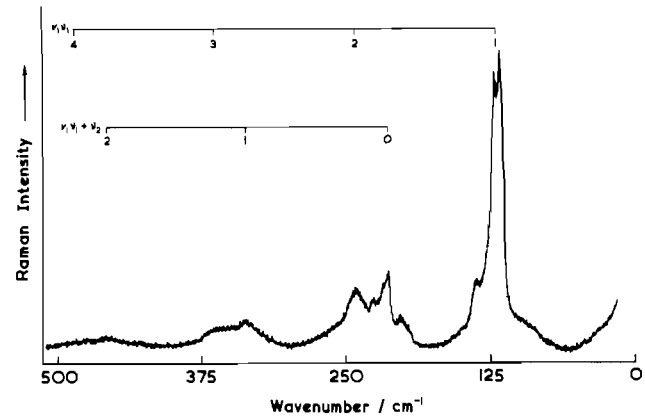

Figure 7. Resonance Raman spectrum of $K_4[Pt_2(pop)_4Br]\cdot 3H_2O$ at ca. 80 K (λ_0 = 676.4 nm, power 15 mW, spectral slit width 1 cm^{-1}).

implying a near-symmetric iodine bridge in the complex. Its wavenumber is only slightly less than that of $[Pt_2(pop)_4I_2]^{4-}$ (189 cm^{-1}). The principal progression-forming mode is ν_1, the PtPt stretching mode at 100 cm^{-1}, which evidently forms the progressions $\upsilon_1\nu_1$ to υ_1 = 5 and $\upsilon_1\nu_1 + \delta$(POP) to υ_1 = 2. For neither the bromide nor the iodide could Raman band excitation profiles be obtained, although all bands are obviously enhanced toward the red; infrared exciting lines would be needed in these cases in order to locate the maxima. The observation that it is ν_1 rather than ν_2 which is the principal progression-forming mode in the case of the bromide and iodide reflects either some degree of changed character to the intervalence (resonant) transition or the progressive change in the mix of a_{1g} symmetry coordinates in the Pt–Pt normal mode on changing from chloride to bromide or iodide, cf. that for $[Pt_2(pop)_4X_2]^{4-}$ ions.[6]

The ν_1 band of $K_4[Pt_2(pop)_4Br]\cdot 3H_2O$ is a doublet at 117 and 122 cm^{-1}, and hence only approximate spectroscopic analyses of the RR progressions are possible. These lead to the values ω_1 = 121 ± 1 cm^{-1} and $x_{11} = -0.4 \pm 0.1$ cm^{-1}. For the analogous iodide, the values ω_1 = 100.5 ± 0.5 cm^{-1} and $x_{11} = -0.3 \pm 0.1$ cm^{-1} were obtained.

Although the dimers $[Pt_2(pop)_4X_2]^{4-}$, as expected, do not give an ESR signal, the chain complexes do display a weak, very broad signal, the intensity of which is increased marginally on lowering the temperature from 295 to 120 K. The signal intensity also increases in the order Cl < Br < I (for the iodide, g = 2.14 at 120 K, ΔH_{pp} = 480 G). The observation of this ESR signal for the complexes is consistent with their $Pt^{II}\cdots Pt^{III}$–X formulation, cf. the similar observations for the related chain complex $[Pt_2(dta)_4I]^{4-}$ (dta = dithioacetate),[19] although the essential diamagnetism of the complexes is presumably accounted for by superexchange or band formation.

Conclusion

It is clear that the chain mixed-valence complexes display many of the properties of Wolffram's-red-type chain complexes. In particular, the chain chloride is a localized-valence species with a very asymmetrically placed chlorine atom. Both the spectroscopic and the crystallographic results indicate that the chain bromide and chain iodide are much more nearly delocalized valence species with nearly symmetrically placed halogen atoms. There is evidently increased mixing of halide character in the order Cl < Br < I in the d_σ Pt–Pt wave functions. The iodo complex has properties and structure very similar to that of $Pt_2(CH_3CS_2)_4I$, which is likewise a diamagnetic semiconductor with an intense, very broad, asymmetric band in the near-infrared region (7900 cm^{-1}) assigned to the intervalence band and with a linear-chain structure containing nearly equal Pt–I bond lengths (2.975 and 2.981 Å).[19]

Acknowledgment. We are indebted to the SERC for financial support, to Johnson-Matthey PLC for the loan of chemicals, and to A. J. Hempleman for recording of the infrared spectra.

(19) Bellito, C.; Flamino, A.; Gastaldi, L.; Scaramuzza, L. *Inorg. Chem.* **1983**, *22*, 444–449.

Registry No. $K_4[Pt_2(pop)_4]$, 80011-26-3; $K_4[Pt_2(pop)_4Cl_2]$, 85335-49-5; $K_4[Pt_2(pop)_4Br_2]$, 82135-55-5; $K_4[Pt_2(pop)_4I_2]$, 85335-50-8; $K_4[Pt_2(pop)_4Cl]$, 85553-26-0; $K_4[Pt_2(pop)_4Br]$, 98875-97-9; $K_4[Pt_2(pop)_4I]$, 85553-25-9.

Contribution from the Institutes of Inorganic Chemistry, University of Frankfurt, Niederurseler Hang, D-6000 Frankfurt (Main) 50, West Germany, and University of Göttingen, Nikolausberg, D-3400 Göttingen, West Germany

Gas-Phase Reactions. 52.[1] Pyrolysis of S_4N_4[§]

HANS BOCK,*[†] BAHMAN SOLOUKI,[†] and HERBERT W. ROESKY[‡]

Received December 21, 1984

The potentially explosive title compound is thermally decomposed in a controlled way by using a flow system under reduced pressure and PE spectroscopic gas analysis. The two reaction channels to 2 SN at lower and to $N_2 + S_2$ at higher temperature are rationalized by semiempirical hypersurface calculations. Our report containing information on both the decomposition conditions and the products formed may be useful for the polymerization to superconducting $(SN)_x$. The interesting dynamics of the S_2N_2 system will hopefully stimulate further theoretical work employing e.g. correlated wave functions.

Tetrasulfur tetranitride, S_4N_4, a cage with a square set of N atoms and a bisphenoid of S atoms, forms thermochromic crystals and must be handled with care, since friction, percussion, or rapid heating can cause it to explode.[2] When this compound is pumped through silver wool heated to 490 K, colorless crystals of square-planar S_2N_2, another explosive,[2,3] can be isolated, which at room temperature polymerize to the golden, lustrous, superconducting $(SN)_x$.[2,3] In the gas phase at pressures below 10^{-2} mbar the following sulfur nitrides have been identified and characterized by their photoelectron spectra: $(SN)_4$,[4a] $(SN)_2$,[4a,b] and SN.[4c] On the basis of above prior knowledge[2-4] and our experience concerning the controlled thermal decomposition[5] of hazardous compounds like azides[1,5,6] in flow systems using PE spectroscopic real-time analysis,[5] we have pyrolyzed S_4N_4 at 10^{-2} mbar pressure and temperatures up to 1100 K (Figure 1).

The PE spectra recorded during the S_4N_4 pyrolysis over silver wool (Figure 1) exhibit a marked temperature dependence: nitrogen evolution starts already at about 800 K, presumably due to the reaction of S_4N_4 with the silver surface to form Ag_2S as the decomposition catalyst.[3] At 900 K all S_4N_4 is converted (Figure 1, peak at 9.36 eV has vanished) predominantly into S_2N_2

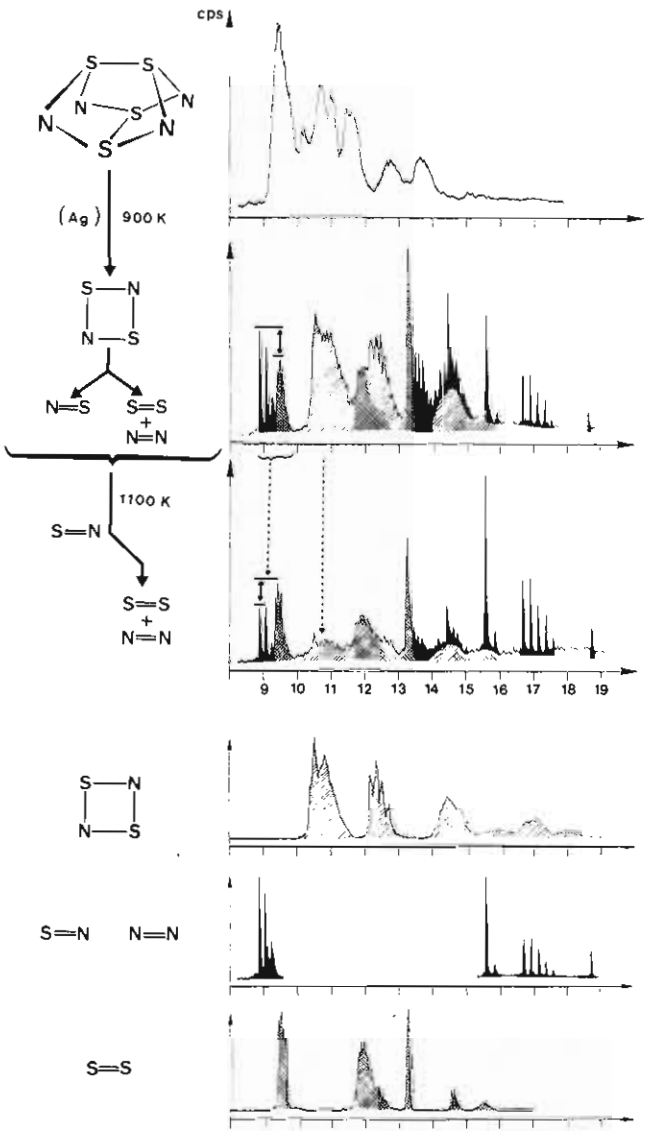

Figure 1. He I PE spectra of S_4N_4, its pyrolysis products formed over silver wool at 900 K and at 1100 K, and reference molecules S_2N_2 (hatched),[4b] SN (black),[4c] N_2 (black), and S_2 (cross-hatched).[7] Instrumentation: Leybold Heraeus UPG 200[5] PE spectrometer equipped with a short-pathway decomposition furnace with additional electron bombardment heating.[8] Calibration: $^2P_{3/2}$ (Ar) at 15.76 eV.

[†] University of Frankfurt.
[‡] University of Göttingen.
[§] Dedicated to Professor M. Schmidt on the occasion of his 60th birthday.

(1) Part 51: Bock, H.; Solouki, B.; Rosmus, P.; Dammel, R.; Hänel, P.; Hierholzer, B.; Lechner-Knoblauch, U.; Wolf, H.-P. "Abstracts of Papers", 7th International Symposium on Organosilicon Chemistry, Kyoto, Japan; Ellis Horwood Ltd.: Chichester, England, 1985; pp 45–74.
(2) Cf. e.g.: Cotton, F. A.; Wilkinson, G. "Advanced Inorganic Chemistry", 4th ed.; Wiley: New York, 1980; pp 515–518, and literature quoted therein.
(3) Mikulski, C. M.; Russo, P. J.; Saran, M. S.; McDiarmid, A. G.; Garito, A. F.; Heeger, A. J. *J. Am. Chem. Soc.* **1975**, *97*, 6358 and literature quoted therein.
(4) (a) Findlay, R. H.; Palmer, M. H.; Downs, A. J.; Egdell, R. G.; Evans, R. *Inorg. Chem.* **1980**, *19*, 1307 and references given especially to numerous other calculations on S_4N_4, S_2N_2, and SN. (b) Frost, D. C.; Le Geyt, M. R.; Paddock, N. L.; Westwood, N. P. *J. Chem. Soc., Chem. Commun.* **1977**, 217. (c) Dyke, J. M.; Morris, A.; Trickle, I. R. *J. Chem. Soc., Faraday Trans. 2* **1977**, *73*, 147.
(5) For a review on "Photoelectron Spectra and Molecular Properties: Real-Time Gas Analysis in Flow Systems", cf.: Bock, H.; Solouki, B. *Angew. Chem.* **1981**, *93*, 425; *Angew. Chem., Int. Ed. Engl.* **1981**, *20*, 427.
(6) Refer to the following references for the compounds mentioned: (a) Methyl azide: Bock, H.; Dammel, R.; Horner, L. *Chem. Ber.* **1981**, *114*, 220. (b) Vinyl azide: Bock, H.; Dammel, R.; Aygen, S. *J. Am. Chem. Soc.* **1983**, *105*, 7681. See also ref 5. (c) Allyl azide: Herrmann, W. A.; Kriechbaum, G. W.; Dammel, R.; Bock, H. *J. Organomet. Chem.* **1983**, *254*, 219. (d) $H_5C_6Si(N_3)_3$: Bock, H.; Dammel, R. *Angew. Chem., Int. Ed. Engl.* **1985**, *24*, 111; *Angew. Chem.* **1985**, *97*, 128.

0020-1669/85/1324-4425$01.50/0